Available online at www.sciencedirect.com
SCIENCE DIRECT®
Chemical Physics Letters 424 (2006) 46–53
CHEMICAL PHYSICS LETTERS
www.elsevier.com/locate/cplett

Accurate MRCI study of ground-state N_2H_2 potential energy surface

M. Biczysko, L.A. Poveda, A.J.C. Varandas *

Departamento de Química, Universidade de Coimbra, 3004-535 Coimbra, Portugal

Received 26 January 2006; in final form 3 April 2006
Available online 28 April 2006

Abstract

Extensive ab initio calculations have been performed to determine the energy, geometry and vibrational frequencies of all stationary points of the N_2H_2 ground-state potential energy surface. The geometries of *trans*-, *cis*- and *iso*-minima as well as transition states are reported at the MCSCF/aug-cc-pVQZ level, while the relative energetics is established by single point MRCI/aug-cc-pVQZ calculations including the Davidson size-consistency correction. The data is useful for modeling a single-sheeted global potential energy surface for the title system.

1. Introduction

It is well known that gas phase hydrogenation of nitrogen can occur without a catalyst only under extreme conditions due to the high energy barriers involved, although a detailed reaction mechanism has not been established yet. It is also accepted [1] that the addition of the first hydrogen molecule to nitrogen is the rate-determining step of the nitrogen hydrogenation process leading to ammonia. Knowledge of an accurate global potential energy surface for N_2H_2 is therefore a key step toward the understanding of the elementary reactions involved in such processes.

There have been several theoretical [1–13] and experimental [14–19] studies of the title system (a more complete list of earlier theoretical and experimental work is given in Refs. [3,2]). Some of these studies focused on the determination of accurate geometries, frequencies and relative stabilities of three local minima: *trans*-, *cis*-, and *iso*-N_2H_2 [3,7,14–19,11,10]. Moreover, there has been considerable theoretical work [2,1,9,4,8,6,5,12,13] on the determination of the barriers involved in the diimide isomerization or formation processes, often for testing the accuracy of theoretical methods that are used to study chemical reactions [13,12,4,6]. All published work agrees on the structures of the above minima (*trans*-, *cis*-, and *iso*-) for N_2H_2, although the agreement for transition states (TSs) stands only for the TS associated to the *trans–iso* conversion. For the other TSs, discrepancies exist between the various theoretical results. In particular, for the *trans–cis* conversion, some papers predict both rotational and inversional reaction paths [2,9,8] while others infer it to occur by inversion [6,12,13] or rotation [1] only.

Regarding previous work on the potential energy surface of N_2H_2 (considering also reaction paths for diazene formation), the most detailed studies have been performed by Jensen et al. [2] at the complete-active-space self-consistent field (CASSCF) level using a basis set of double-ζ quality and more recently by Hwang and Mebel [1] using G2M(MP2)//MP2/6-31G** theory. The CASSCF calculations [2] predict three more transition states on the N_2H_2 potential energy surface, in addition to the *trans–cis* and *trans–iso* isomerization processes. They are associated to the dissociative ($N_2H + H$) transition state, a C_{2v} TS where both NH bonds are elongated in comparison to the *cis*-minimum (obtained by walking along the symmetric stretching or bending coordinates from *cis*-N_2H_2), and a TS for N_2H_2 (isodiazene) formation from $N_2 + H_2$. On the other hand, the G2M(MP2)//MP2/6-31G** calculations of Hwang and Mebel [1] predict two transition states for diazene formation from hydrogen and nitrogen mole-

* Corresponding author. Fax: +351 239 835867.
E-mail addresses: bicz@kn.pl (M. Biczysko), varandas@qtvs1.qui.uc.pt (A.J.C. Varandas).

0009-2614/$ - see front matter © 2006 Elsevier B.V. All rights reserved.
doi:10.1016/j.cplett.2006.04.073

cules leading to *cis*- and *iso*-N_2H_2, but only one (rotational) reaction path for *trans–cis* isomerization. Instead of the inversional path (reported by other studies performed at G2 level [6,12]), a transition state corresponding to *trans*-N_2H_2 isomerization by in-plane scrambling of the hydrogen atoms is predicted. Moreover, there are significant discrepancies in the relative energies of several stationary points throughout the literature showing that the potential energy diagram and involved reaction pathways on the ground-state potential energy surface of N_2H_2 are far from well established. This has been a major motivation for carrying out the systematic high level ab initio studies reported in the present work, which employ multireference approaches with extensive basis sets. In fact, our calculations provide also an accurate ground for ongoing work on modeling a global single-sheeted potential energy surface for the title system using double many-body expansion (DMBE; Ref. [20], and references therein) theory.

The paper is organized as follows: Section 2 describes the ab initio calculations carried out in the present work, while the results are discussed in Section 3. The concluding remarks are in Section 4.

2. Ab initio calculations

All structures have been optimized at the multiconfiguration self-consistent field (MCSCF) [21] level using the full valence complete active space (FVCAS) [22] wave function as the reference. This involves 12 correlated electrons distributed over 10 active orbitals. For the basis set we have selected the aug-cc-pVXZ (X = D, T, Q) of Dunning [23,24] (AVXZ) in order to establish an adequate level of theory for modeling the title potential energy surface. Geometry optimizations have been followed by harmonic frequency calculations to confirm the nature of the stationary points (minima and transition states of index one, i.e., having just one imaginary frequency). Reaction paths from all TSs have also been determined by using the Quadratic Steepest Descent (QSD) reaction path following procedure [25]. For all stationary points, single point calculations at the multireference configuration interaction (MRCI) [26] level have been performed in order to obtain accurate relative energies. Moreover, the Davidson [27] (+Q) and Pople [28] (P) size-consistency corrections have been applied. The energies have been subsequently corrected for zero-point energy (ZPE) based on MCSCF frequency calculations. All ab initio calculations employed the MOLPRO [29] package.

3. Results and discussion

The geometries and harmonic frequencies of the *trans*-, *cis*-, and *iso*-N_2H_2 minima calculated at the MCSCF/aug-cc-pVXZ (X = D, T, Q) levels are collected in Table 1. Also given in this Table are the energies obtained from single point MRCI/aug-cc-pVXZ energy calculations including the Davidson size-consistency and zero-point energy corrections (from harmonic calculations at the corresponding MCSCF/AVXZ level). For all minima, there are several theoretical [1–3] and a few experimental [14,16,17] results that may serve for comparison purposes, and hence for establishing the level of theory that is required for subsequent studies of the N_2H_2 potential energy surface. As the most accurate theoretical results reported thus far stand the benchmark calculations of Martin and Taylor [3] using the coupled-cluster, CCSD(T), method with extrapolation to the basis set limit and inclusion of inner-shell correlation effects and anharmonicity in the zero-point energy. We observe an important overall improvement in the calculated optimized geometries when going from AVDZ to AVTZ, with a further improvement of the basis set to AVQZ quality giving an even better agreement with the reference data [3]. For bond lengths the associated average discrepancies are 0.034, 0.022 and 0.021 a_0 for the AVDZ, AVTZ, and AVQZ basis sets (respectively), while the corresponding maximum deviations are 0.048, 0.034, and 0.033 a_0. For the angles, the average discrepancy varies from more than 0.5° for the AVDZ basis set to 0.41° for AVTZ, and 0.36° for AVQZ. No significant improvement is observed for the frequencies. However, the maximum discrepancies do not exceed 150 cm^{-1}, and hence may be considered relatively small, especially having in mind that the effect of anharmonicity has not been included in the present work. In fact, the most important sign of having attained good accuracy refers to the energetics. Indeed, the MRCI + Q/AVTZ and MRCI + Q/AVQZ corrected for zero-point energies (ZPEs) from this work are shown to differ by less than 0.2 kcal mol^{-1} from the best theoretical estimates [3], with slightly better agreement in case of the AVQZ basis set (average errors of 0.1 and 0.08 kcal mol^{-1} for AVTZ and AVQZ basis sets, respectively). We have also extrapolated the dynamical correlation energy to the basis set limit [30], but observed no significant improvement in the relative energetics of the three minima. This seems to indicate that the energy calculations here reported are fairly well converged at the MRCI + Q/aug-cc-pVQZ level.

The accuracy of the calculations of the present work may further be assessed by comparing with the results of Hwang and Mebel [1] and Jensen et al. [2] which represent the most extensive studies of stationary points on the global potential energy surface of N_2H_2 carried out thus far. In both studies [1,2] the bond lengths are overestimated by up to 0.04 a_0, and the frequencies by up to more than 300 cm^{-1}. As for the relative energies, the agreement with the best reported estimate [3] is of 0.5 kcal mol^{-1} in the case of Hwang and Mebel [1], while the relative energies of Jensen et al. [2] for the *cis* and *iso* isomers are found to be overestimated by 1.47 kcal mol^{-1} and 10.47 kcal mol^{-1}, respectively. In turn, a comparison of the local minima of diazene reported in the present work with those from previous studies for the title system [1,2] including the best theoretical estimates of Martin and Taylor [3] suggest that they may stand as accuracy tests for subsequent studies

Table 1
Properties of local minima for N_2H_2

Feature	Property	MRCI + Q/AVDZ// MCSCF/AVDZ[a]	MRCI + Q/AVTZ// MCSCF/AVTZ[a]	MRCI + Q/AVQZ// MCSCF/AVQZ[a]	G2M(MP2)// MP2/6-31G*[b]	CASSCF[c]	CCSD(T)/ VQZ[d]	Experimental
Global minimum *trans*-N_2H_2	R_{NN} (a_0)	2.3897	2.3767	2.3741	2.3943	2.3924	2.3561	2.3565[e]
	R_{NH} (a_0)	1.9821	1.9702	1.9688	1.9502	1.9748	1.9428	1.9464[e]
	∠HNN (°)	105.6	105.9	106.0	105.1	104.8	106.2	106.3[e]
	ω_1(N–N)/cm^{-1}	1540	1527	1530	1525	1526	1528	1529[f]
	ω_2(N–H)$_{sym}$/cm^{-1}	3122	3124	3131	3382	3154	3051	3128[f]
	ω_3(N–H)$_{asym}$/cm^{-1}	3152	3158	3164	3353	3197	3133	3120[f], 3120.29[g]
	ω_4(N–N–H)$_{sym}$/cm^{-1}	1616	1617	1619	1628	1663	1578	1582[f]
	ω_5(N–N–H)$_{asym}$/cm^{-1}	1351	1354	1355	1360	1374	1317	1322[f], 1316.41[g]
	ω_6(tors)/cm^{-1}	1314	1321	1323	1349	1351	1294	1286[f],1288.65[g]
	ΔE/kcal mol^{-1}	0.0	0.0	0.0	0.0	0.0	0.0	
cis-N_2H_2	R_{NN} (a_0)	2.3804	2.3732	2.3710	2.3829	2.3924	2.3538	
	R_{NH} (a_0)	2.0006	1.9807	1.9791	1.9596	1.9748	1.9523	
	∠HNN (°)	111.5	111.6	111.7	111.9	104.8	111.9	
	ω_1(N–N)/cm^{-1}	1571	1545	1548	1562	1535	1548	1558[h]
	ω_2(N–H)$_{sym}$/cm^{-1}	3035	3088	3092	3306	3144	3003	2966[h]
	ω_3(N–H)$_{asym}$/cm^{-1}	2940	2997	3002	3225	3074	2987	2884[h]
	ω_4(N–N–H)$_{sym}$/cm^{-1}	1368	1358	1359	1373	1416	1335	1390[h]
	ω_5(N–N–H)$_{asym}$/cm^{-1}	1573	1579	1580	1567	1616	1521	1439[h]
	ω_6(tors)/cm^{-1}	1254	1255	1258	1287	1267	1232	1259[h]
	ΔE/kcal mol^{-1}	5.35	5.09	5.05	4.81	6.68	5.21	
iso-N_2H_2	R_{NN} (a_0)	2.3140	2.2991	2.2968	2.3092	2.3130	2.3002	
	R_{NH} (a_0)	1.9973	1.9886	1.9875	1.9634	1.9615	1.9544	
	∠ HNN (°)	124.1	124.2	124.2	124.1	124.4	123.5	
	ω_1(N–N)/cm^{-1}	1603	1588	1590	1664	1611	1560	1574[i]
	ω_2(N–H)$_{sym}$/cm^{-1}	2916	2906	2910	3173	2868	2770	2805[i]
	ω_3(N–H)$_{asym}$/cm^{-1}	2943	2944	2946	3211	3253	2867	2862[i]
	ω_4(sciss)/cm^{-1}	1727	1737	1739	1783	1814	1665	1645[i]
	ω_5(rock)/cm^{-1}	1330	1341	1346	1364	1375	1293	1288[i]
	ω_6(tors)/cm^{-1}	1012	1014	1018	1060	1039	991	1003[i]
	ΔE/kcal mol^{-1}	25.23	24.31	24.04	24.65	34.59	24.12	

[a] Energies from this work calculated at MRCI + Q/aug-cc-pVXZ level for MCSCF/aug-cc-pVXZ optimized structures that have been corrected for ZPE using MCSCF/aug-cc-pVXZ frequency calculations; see text.
[b] G2M(MP2) energies for MP2/6-31G** optimized structures from Hwang and Mebel [1].
[c] Energies corrected for ZPE from Jensen et al. [2].
[d] Best estimate at 0 K accounting for inner-shell correlation and anharmonic ZPE corrections from Martin and Taylor [3].
[e] Ref. [14].
[f] Ref. [16].
[g] Ref. [15].
[h] Estimates from Creig and Levin [16] based on approximate force field of *trans*-N_2H_2.
[i] Ref. [17].

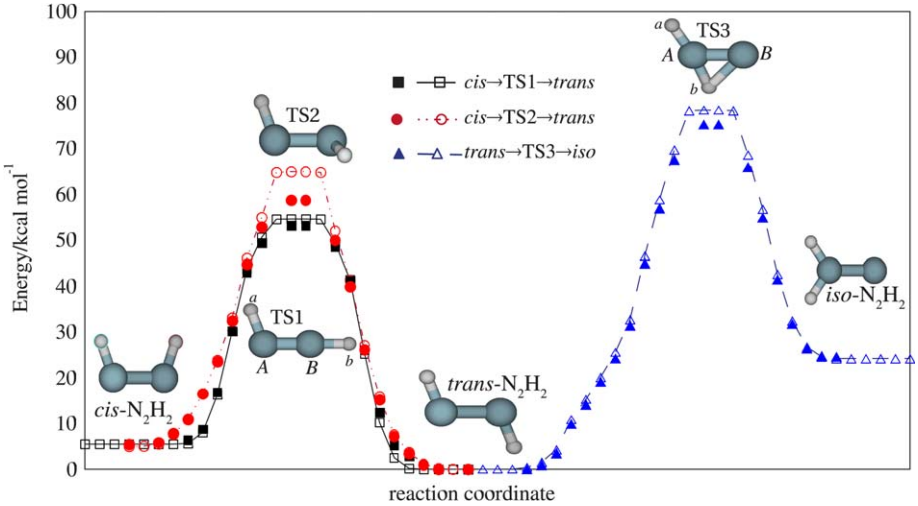

Fig. 1. Reaction path following calculations performed at MCSCF/aug-cc-pVQZ level for the isomerizations between local minima: squares and solid black line *trans–cis* path through inversional (TS1) transition state; circles and dash-dot red line, *trans–cis* path through rotational (TS2) transition state; triangles and dashed blue line, *trans–iso* path. Selected points on reaction paths calculated at MRCI + Q/aug-cc-pVQZ level are shown by solid symbols. When appropriate in this and subsequent figures, the nitrogen (hydrogen) atoms are distinguished by using the labels *A* and *B* (*a* and *b*). Energies are in kcal mol^{-1} relative to the *trans*-N_2H_2 minimum. (For interpretation of the references in colour in this figure legend, the reader is referred to the web version of this article.)

of other stationary points on the N_2H_2 potential energy surface. Thus, our work suggests that geometries and vibrational frequencies of transition states from MCSCF/aug-cc-pVQZ calculations, with the energetics determined from single point computations at the MRCI + Q/aug-cc-pVQZ level corrected for ZPE, provide the best theoretical estimates reported thus far for the N_2H_2 system.

For the TS calculations, we have considered all structures reported in literature as starting points for the symmetry unconstrained geometry optimizations at the MCSCF/AVQZ level. In the case of the TS3 of Jensen et al. [2] (C_{2v} structure with both NH bonds elongated in comparison to the *cis*-minimum), it leads to the dissociative (N_2H + H) transition state TS6. When starting at the TSt-t of Hwang and Mebel [1] (C_{2h} structure with both NNH angles close to 180°), the transition state search carried out in the present work terminated at TS1. It should be added though that the actual structure has not been reported in Ref. [1]. Moreover, for all transition states, reaction path following calculations using the QSD [25]

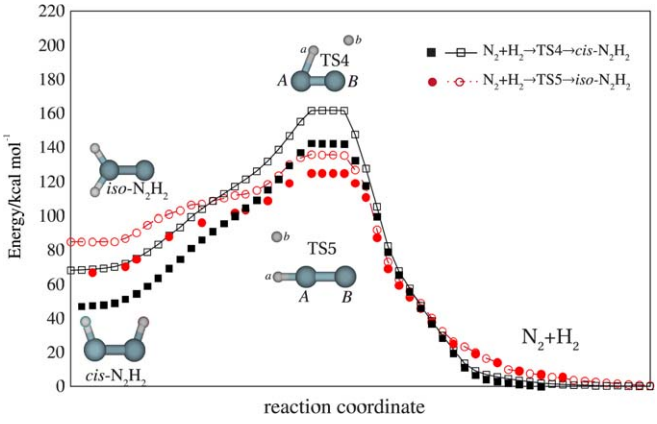

Fig. 2. Reaction paths for formation of N_2H_2 from molecular nitrogen and hydrogen. TS4 and TS5 are transition states for the parallel (squares and solid black line) and perpendicular (circles and dashed red line) approaches of N_2 and H_2, respectively. Reaction path following calculations have been performed at MCSCF/aug-cc-pVQZ level and followed by MRCI + Q/aug-cc-pVQZ calculations for selected points (solid symbols). Energies are in kcal mol^{-1} relative to the $N_2 + H_2$ asymptote. (For interpretation of the references in colour in this figure legend, the reader is referred to the web version of this article.)

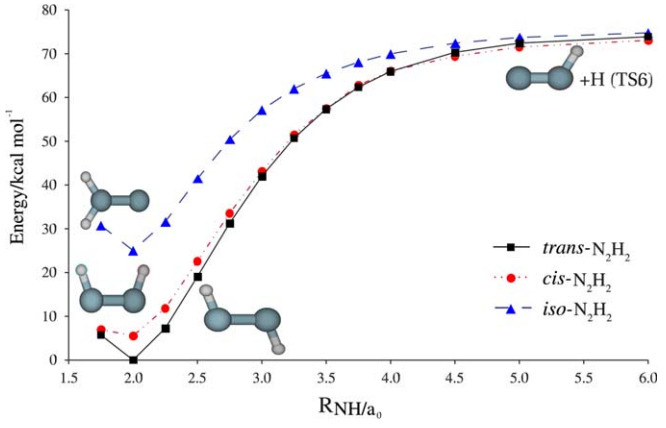

Fig. 3. The dissociation–recombination pathways leading to the N_2H + H (TS6). Energy profiles for the dissociation of one hydrogen atom from the *trans*- (squares and solid black line), *cis*- (circles and dash-dot red line) and *iso*-N_2H_2 (triangles and dashed blue line) are calculated at the MRCI + Q/aug-cc-pVQZ level. For all structures, the NN distance and other NH distance have been fixed at 2.35 a_0 and 2.0 a_0 respectively, while the angles have been kept at the values corresponding to the optimized structures of *trans*-, *cis* and *iso* minima. Energies are in kcal mol^{-1} relative to the *trans*-N_2H_2 minimum. (For interpretation of the references in colour in this figure legend, the reader is referred to the web version of this article.)

Table 2
Properties of transition states of N_2H_2 system

Feature	Property	MRCI + Q/AVQZ// MCSCF/AVQZ[a]	G2M(MP2)// MP2/6-31G*[b]	CASSCF[c]	G2M(MP2)// DFT/DZVP[d]
TS1	R_{NN} (a_0)	2.3299		2.3622	2.3300
	$R_{N_AH_a}$(a_0)	2.0155		2.0126	2.0390
	$R_{N_BH_b}$(a_0)	1.8514		1.8708	1.9011
	$\angle H_aN_AN_B$ (°)	110.5		108.1	109.5
	$\angle H_bN_BN_A$ (°)	178.4		178.9	177.4
	ΔE/kcal mol^{-1}	51.07		63.35	49.53
	Frequencies/cm^{-1}	1720*i*		2075*i*	1509*i*
		678		684	682
		1513		1536	1448
		1626		1614	1691
		2733		2876	2701
		4053		3957	3812
TS2	R_{NN} (a_0)	2.5546	2.4812	2.6645	
	R_{NH} (a_0)	1.9854	1.9521	1.9974	
	$\angle$HNN (°)	107.5	110.0	103.4	
	θ (°)	91.4	90.0	89.9	
	ΔE/kcal mol^{-1}	54.96	48.86	62.93	
	Frequencies/cm^{-1}	4802*i*	1328*i*	3323*i*	
		961	964	923	
		1192	1117	1257	
		1218	1306	1279	
		2980	3341	2991	
		2995	3357	3001	
TS3	R_{NN} (a_0)	2.4399	2.4359	2.4548	2.4207
	$R_{N_AH_a}$(a_0)	2.0134	1.9804	2.0144	2.0409
	$R_{N_AH_b}$(a_0)	2.1091	2.0541	2.0598	2.1203
	$R_{N_BH_b}$(a_0)	2.5682	2.5738	2.5833	2.5795
	$\angle H_aN_AN_B$ (°)	121.3	120.0	122.1	121.1
	ΔE/kcal mol^{-1}	70.87	71.07	81.76	70.26
	Frequencies/cm^{-1}	2302*i*	2423*i*	2186*i*	1953*i*
		559	636	574	652
		1325	1359	1330	1319
		1467	1541	1513	1503
		2594	2918	2625	2605
		2888	3203	3082	2882
TS4	R_{NN} (a_0)	2.2852	2.3017		
	$R_{N_AH_a}$(a_0)	2.3345	2.3395		
	$R_{N_BH_b}$(a_0)	3.2210	2.9234		
	R_{HH} (a_0)	2.5748	2.3622		
	$\angle H_aN_AN_B$ (°)	63.5	61.2		
	ΔE/kcal mol^{-1}	92.94	95.55		
	Frequencies/cm^{-1}	3363*i*	3234*i*		
		756	850		
		859	1041		
		941	1303		
		1592	1743		
		2217	2447		
TS5	R_{NN} (a_0)	2.1607	2.1845	2.1807	
	$R_{N_AH_a}$(a_0)	1.9180	1.9067	1.8765	
	$R_{N_AH_b}$(a_0)	3.4085	3.3562	3.3996	
	R_{HH} (a_0)	2.9604	2.8818	2.9298	
	$\angle H_bN_AN_B$ (°)	123.9	126.1	124.6	
	$\angle H_aN_AN_B$ (°)	176.1	174.9	176	
	ΔE/kcal mol^{-1}	74.15	76.32	78.77	
	Frequencies/cm^{-1}	2024*i*	2001*i*	2387*i*	
		716	728	713	
		720	792	742	
		1216	1261	1240	
		1827	2136	1892	
		3520	3725	3831	

Table 2 (*continued*)

Feature	Property	MRCI + Q/AVQZ// MCSCF/AVQZ[a]	G2M(MP2)// MP2/6-31G*[b]	CASSCF[c]	G2M(MP2)// DFT/DZVP[d]
$N_2H + H$(TS6)	R_{NN} (a_0)	2.2313	2.1751	2.2469	
	R_{NH} (a_0)	2.0395	1.9842	2.0674	
	∠ HNN (°)	116.0	120.9	112.4	
	ΔE/kcal mol^{-1}	61.22	63.6	54.2	
	Frequencies/cm^{-1}	1121	1050	1141	
		1714	2895	1614	
		2425	3015	2247	

[a] This work. Energies obtained from single point MRCI + Q/aug-cc-pVQZ calculations for MCSCF/aug-cc-pVQZ optimized structures, and corrected for ZPE based on MCSCF/aug-cc-pVQZ frequency calculations; see text.
[b] G2M(MP2) energies for MP2/6-31G** optimized structures from Hwang and Mebel [1].
[c] Energies corrected for ZPE from Jensen et al. [2].
[d] Structures calculated [13] using density functional theory (DFT), and energies from G2M(MP2) theory [12].

scheme have been performed at the MCSCF/aug-cc-pVQZ level, which were followed by single point MRCI + Q/aug-cc-pVQZ energy calculations at selected reaction steps. The reaction paths connecting *trans*-N_2H_2 to the *cis* and *iso* isomers are shown in Fig. 1, while the energy profiles for the N_2H_2 formation from molecular hydrogen and nitrogen are shown in Fig. 2. In turn, Fig. 3 relates to the dissociation–recombinations reaction paths via $N_2H + H$ (TS6). The potential energy scan for dissociation of a hydrogen atom from *trans*-, *cis*-, and *iso*-N_2H_2 has been calculated at the MRCI + Q/aug-cc-pVQZ level of theory. These figures collect all the structures of minima and transition states of N_2H_2 found in the present study, while Table 2 compares the transition states geometries, frequencies and relative energies with data from other theoretical works [1,2,13,12].

There has been a dispute in the literature on whether the *trans–cis* isomerization occurs via one or two transition states connecting these structures (inversional-TS1 or rotational-TS2) or rather that all rearrangements within the N_2H_2 system evolve through the dissociation–recombination pathway involving TS6. The first theoretical works (see Ref. [9]) predicted the inversional mechanism to be favored over the rotational one, with the possibility of dissociative rearrangement having been excluded [9] based on the activation energies of related processes. More recent calculations using CASSCF [2] and G2M [1,12,6] methods predict very similar stabilities for TS1 and TS2, with TS2 being favored by less than 1 kcal mol^{-1}. Moreover, CASSCF calculations [2] predict TS6 to be significantly lower in energy than both TS1 and TS2, but recombination after dissociation has been ruled out due to the instability of the N_2H radical. In this study, we have confirmed that multireference SCF calculations (see Table 3) predict TS6 to lie lowest in energy. However, when MRCI calculations are performed, TS6 is encountered to lie above both TS1 and TS2 by 10.15 kcal mol^{-1} and 6.25 kcal mol^{-1}, respectively. Moreover, our calculations predict the inversional barrier to be slightly lower than the rotational one, although their relative positions calculated at MRCI level differ by less than 5 kcal mol^{-1}. Note that TS2 has a high imaginary frequency, which may enhance the possibility of reaction via a tunneling mechanism through the rotational path. Thus, our results suggest that the dissociative reaction path can be ruled out for the *trans–cis* isomerization. Yet, because the N_2H radical has been found to be a metastable species [31–33], TS6 can be relevant in other recombination processes of N_2H_2.

For the *trans–iso* isomerization, all theoretical studies [1,12,6,2,9] reported only one transition state, namely TS3. Moreover, its energy has been predicted to be about 70 kcal mol^{-1} relative to the *trans* isomer, thus significantly above TS6. As a result, such an isomerization may most likely occur via a dissociation–recombination pathway.

For TS4 and TS5, it has been found that both structures are transition states of index one for the formation of N_2H_2 from molecular nitrogen and hydrogen. The perpendicular approach leading to *iso*-N_2H_2 via TS5 is favorable in comparison to the parallel approach leading to *cis*-N_2H_2 via TS4. However, in both cases barriers of more than 120 kcal mol^{-1} relative to the $N_2 + H_2$ dissociation limit are involved.

As mentioned in the Introduction, this paper stands as a first step toward the modeling of a global DMBE potential energy surface for the title system from accurate ab initio calculations. Thus, energies of all stationary points of N_2H_2 and possible dissociative limits have been calculated at different levels of theory, being collected in Table 3 along with the best theoretical and experimental estimates. As benchmark for the accuracy of relative energies stands the heat of formation of *trans*-N_2H_2 (48.8 ± 0.5 kcal mol^{-1}), recently established with good accuracy [19]. To compare with this experiment, theoretical thermochemical data should be used, although it has already been shown for the title system [10] that CI calculations are necessary to reach good agreement between computed and experimental enthalpies. In this work, instead of extremely expensive calculations of enthalpies at MRCI/aug-cc-pVQZ level that would be required for such a purpose, we compare the energies obtained from MCSCF and MRCI calculations subsequently corrected for zero-point energy by using frequencies at the MCSCF/aug-cc-pVQZ level. For the MRCI we consider also energies corrected for size-consistency according to the Pople [28] and David-

Table 3
Stationary points on N_2H_2 potential energy surface

	MCSCF/AVQZ//MCSCF/AVQZ[a]	MRCI/AVQZ//MCSCF/AVQZ[a]	MRCI(P)/AVQZ//MCSCF/AVQZ[a]	MRCI + Q/AVQZ//MCSCF/AVQZ[a]	G2M(MP2)//MP2/6-31G*[b]	CASSCF[c]	CCSD(T)/cc-pV∞Z[d]	Experimental
trans-N_2H_2	0.00	0.00	0.00	0.00	0.00	0.00	0.00	0[e]
cis-N_2H_2	4.60	5.03	5.05	5.05	4.81	6.68	5.21	
iso-N_2H_2	23.40	24.02	24.04	24.04	24.65	34.59	24.12	
TS1	54.29	51.40	51.11	51.07	49.53[g]	63.35		
TS2	61.03	56.39	55.09	54.96	48.86	62.93		
TS3	73.72	71.44	70.93	70.87	71.07	81.76		
TS4	90.50	93.16	92.95	92.94	95.55			
TS5	68.42	74.15	74.13	74.15	76.32	78.77		
N_2H + H(TS6)	49.36	59.94	61.08	61.22	63.6	54.20		
N_2 + 2H	18.61	48.56	52.48	52.96		18.34		
NH + NH	107.30	119.00	118.86	118.88	124.83			121.6[f]
$NH_2(^2A'') + N(^2D)$	156.39	162.13	161.33	161.28				
$2N(^4S) + 2H$	234.21	271.13	273.11	273.42			278.73	
$H_2 + 2N(^2D)$	143.59	169.54	169.93	170.06				
NH···NH (van der Waals)	106.63	117.74	117.54	117.56				
$N_2 + H_2$	−70.80	−52.75	−50.30	−50.01	−48.88	−72.44	−49.57	−48.8[e]

Energies are in kcal mol^{-1} relative to the *trans*-N_2H_2 minimum.

[a] This work. Energies from single point MRCI + Q/aug-cc-pVQZ calculations for MCSCF/aug-cc-pVQZ optimized structures, and corrected for ZPE based on MCSCF/aug-cc-pVQZ frequency calculations; see text.

[b] G2M(MP2) energies for MP2/6-31G** optimized structures from Hwang and Mebel [1].

[c] Energies corrected for ZPE from Jensen et al. [2].

[d] Best estimate at 0 K accounting for inner-shell correlation and anharmonic ZPE corrections from Martin and Taylor [3].

[e] Ref. [19].

[f] Values obtained from experimental atomization energies [1].

[g] Ref. [12].

son [27] schemes. The MCSCF calculations can be found to fail drastically in predictions of relative energies, as compared to the MRCI + Q results, with average errors of 0.4, 5.7, and 22.9 kcal mol^{-1} for local minima, transition states and dissociative limits, respectively. The situation remains unchanged if enthalpy calculations (not reported here) are considered. Moreover, MRCI energies corrected only for ZPE still give results of unsatisfactory accuracy for relative energies, with the heat of formation of *trans*-N_2H_2 overestimated by 4 kcal mol^{-1}. Conversely, MRCI energies corrected for both size-consistency and zero-point energy agree within chemical accuracy (1 kcal mol^{-1}) with the best experimental [19] estimates and also with the benchmark theoretical results of Martin and Taylor [3] where additional inner-shell correlation and anharmonic ZPE corrections have been taken into account. From these slightly better overall agreement is reached if the Davidson correction is applied. Thus, grid points calculated at the MRCI/aug-cc-pVQZ theory with energies subsequently corrected according to the Davidson scheme should be recommended when aiming at accurate global modeling of the N_2H_2 potential energy surface.

4. Concluding remarks

We have investigated the potential energy surface of N_2H_2 by using multireference approaches at FVCAS and MRCI levels with aug-cc-pVXZ (X = D, T, Q) basis sets. It has been shown that geometries and relative, ZPE corrected, energies of all local minima calculated at MRCI + Q/AVTZ or MRCI + Q/AVQZ levels agree well with the best theoretical estimates. For the barriers involved in the diimide isomerization, this work has confirmed the structures of three transitions states, associated to *trans–cis*(TS1,TS2) and *trans–iso*(TS3) pathways. The possibility of diazene rearrangement via dissociation of one of the hydrogens (TS6) has been ruled out for the former but should be considered for the latter. For N_2H_2 formation from molecular nitrogen and hydrogen, the perpendicular approach leading to *iso*-N_2H_2 via TS5 has been found to be favored over the parallel approach leading to *cis*-N_2H_2 via TS4. Moreover, based on a comparison with the best reported theoretical [3] and experimental [14,19] results, MRCI/aug-cc-pVQZ theory (and possibly the less expensive MRCI/aug-cc-pVTZ one at some regions of configurational space) with energies corrected using the Davidson scheme emerges as the recommended route for modeling the global N_2H_2 potential energy surface.

Acknowledgements

This work has been carried out within Research Training Network HPRN-CT-2002-00170 (Predicting Catalysis), financed by the European Commission. It has also the support of Fundação para a Ciência e a Tecnologia, Portugal,

under program POCI 2010 (contracts QUI/60501/2004, AMB/60261/2004, and REEQ/128/QUI/2005). The authors are also grateful to the Wroclaw Centre for Networking and Supercomputing for computer resources.

References

[1] D.-Y. Hwang, A.M. Mebel, J. Phys. Chem. A 107 (2003) 2865.
[2] H.J.A. Jensen, P. Jorgensen, T. Helgaker, J. Am. Chem. Soc. 109 (1987) 2895.
[3] J.M.L. Martin, P.R. Taylor, Mol. Phys. 96 (1999) 681.
[4] P. Mach, J. Masik, J. Urban, I. Hubac, Mol. Phys. 94 (1998) 173.
[5] S.P. Walch, J. Chem. Phys. 91 (1989) 389.
[6] B.S. Jursic, Chem. Phys. Lett. 261 (1996) 13.
[7] V. Stepanic, G. Baranovic, Chem. Phys. 254 (2000) 151.
[8] L.G. Spears Jr., J.S. Hutchinson, J. Chem. Phys. 88 (1988) 240.
[9] C.J. Casewit, W.A. Goddard III, J. Am. Chem. Soc. 102 (1980) 4057.
[10] U. Brandemark, P.E.M. Siegbahn, Theor. Chim. Acta 66 (1984) 217.
[11] J.A. Pople, L.A. Curtiss, J. Chem. Phys. 95 (1991) 4385.
[12] B.J. Smith, J. Phys. Chem. 97 (1993) 10513.
[13] J. Andzelm, C. Sosa, R.A. Eades, J. Phys. Chem. 97 (1993) 4664.
[14] J. Demaison, F. Hegelund, H. Burger, J. Molec. Struct. 413–414 (1997) 447.
[15] F. Hegelund, H. Burger, O. Polanz, J. Mol. Spectrosc. 167 (1994) 1.
[16] N.C. Craig, I.W. Levin, J. Chem. Phys. 71 (1979) 400.
[17] J.H. Teles, G. Maier, B.A. Hess Jr., L.J. Schaad, Chem. Ber. 122 (1989) 749.
[18] A.P. Sylwester, P.B. Derwan, J. Am. Chem. Soc. 106 (1984) 4648.
[19] H. Biehl, F. Stuhl, J. Chem. Phys. 100 (1994) 141.
[20] A.J.C. Varandas, in: Modeling and Interpolation of Global Multi-sheeted Potential Energy SurfacesAdvanced Series in Physical Chemistry, World Scientific Publishing, 2004, p. 91.
[21] H.-J. Werner, P.J. Knowles, J. Chem. Phys. 82 (1985) 5053.
[22] P.J. Knowles, H.-J. Werner, Chem. Phys. Lett. 115 (1985) 259.
[23] T.H. Dunning, J. Chem. Phys. 90 (1989) 1007.
[24] R. Kendall, T. Dunning Jr., R. Harrison, J. Chem. Phys. 96 (1992) 6769.
[25] J. Sun, K. Ruedenberg, J. Chem. Phys. 99 (1993) 5269.
[26] H.-J. Werner, P.J. Knowles, J. Chem. Phys. 89 (1988) 5803.
[27] S.R. Langhoff, E.R. Davidson, Int. J. Quantum Chem. 8 (1974) 61.
[28] J.A. Pople, R. Seeger, R. Krishnan, Quantum Chem. Symp. 11 (1977) 149.
[29] H.-J. Werner, P.J. Knowles, MOLPRO is a package of ab initio programs written by H.-J. Werner, P.J. Knowles, with contributions from J. Almlöf, R.D. Amos, M.J.O. Deegan, S.T. Elbert, C. Hampel, W. Meyer, K.A. Peterson, R. Pitzer, A.J. Stone, P.R. Taylor, R. Lindh, 1998.
[30] A.J.C. Varandas, J. Chem. Phys. 113 (2000) 8880.
[31] H. Koizumi, G.C. Schatz, S.P. Walch, J. Chem. Phys. 95 (1991) 4130.
[32] L.A. Poveda, A.J.C. Varandas, J. Phys. Chem. 107 (2003) 7923.
[33] P.J.S.B. Caridade, S.P.J. Rodrigues, F. Sousa, A.J.C. Varandas, J. Phys. Chem. A 109 (2005) 2356.